

UNCLASSIFIED

Defense Technical Information Center  
Compilation Part Notice

ADP012399

TITLE: Study on IR and UV - Lasers Interaction with Metal Surfaces

DISTRIBUTION: Approved for public release, distribution unlimited

This paper is part of the following report:

TITLE: Gas and Chemical Lasers and Intense Beam Applications III Held  
in San Jose, CA, USA on 22-24 January 2002

To order the complete compilation report, use: ADA403173

The component part is provided here to allow users access to individually authored sections of proceedings, annals, symposia, etc. However, the component should be considered within the context of the overall compilation report and not as a stand-alone technical report.

The following component part numbers comprise the compilation report:

ADP012376 thru ADP012405

UNCLASSIFIED

## Study on IR and UV - lasers interaction with metal surfaces

Victor F. Tarasenko\*, Sergey B. Alekseev, Andrey V. Fedenev, Igor' M. Goncharenko,  
Nikolay N. Koval', Konstantin V. Oskomov, Victor M. Orlovskii,  
Nikolay S. Sochugov, Mikhail A. Shulepov

High Current Electronics Institute, Siberian Division of the Russian Academy of Sciences  
(HCEI SB RAS)

### ABSTRACT

The complex of experimental installations for studying of laser radiation interaction with surface of metals has been established. At titanium surface irradiating depending on the accumulated laser radiation energy, the surface color might be changed from bright yellow to red and deep-blue colors. The presented results testify to the possibility to use the change of titanium surface color at heating by laser irradiation in the open air to obtain dot raster images (even colored ones). Presently, from the world data available on interaction of laser radiation with metal and dielectric surfaces and development of experimental diagnostics techniques by itself it is allowed to raise a reverse question, i.e., restoration of laser radiation energy spatial distribution through surface imprint. Using imprints, it is also possible to make an express diagnostics of multi-layer surface coatings. With this in mind, we have made the detailed morphology of imprint of the pulsed HF-laser interaction with carbon steel surface through atomic force microscope.

**Keywords:** titanium oxide, laser treatment, laser interaction with surface

### 1. INTRODUCTION

The harnessing of laser irradiation for surface treatment has been practically made at once as the first lasers were developed. Both the gas discharge IR lasers on CO<sub>2</sub> molecule transitions and solid-state Nd:YAG lasers have gained major application in this field<sup>1</sup>. CO<sub>2</sub>-based laser with high efficiency and specific output parameters has a comparatively big wavelength and limited gas mixture lifetime. The Nd:YAG laser also has a high efficiency and it provides operation both in continuous and pulsed repetition modes (up to 100 kHz), but active medium scaling is rather poor. In this paper, preliminary results on lasers interaction with metal surfaces for recently developed lasers, i.e. non-chain gas discharge HF laser and Xe laser pumped by e-beam preionized electric discharge are presented. As objects for study, thin titanium foils and carbon steel samples (0.4% C, 0.8 – 1.0 % Cr, 4140(USA)) were taken.

Titanium oxide coatings attract particular interest in a row of applications such as optical coatings, decorative coatings, catalysts, medical implantates and gas sensors. A good technique to produce such coatings is laser irradiation of metallic titanium surface in reactive atmosphere<sup>2</sup>. As it is presented by authors<sup>2</sup>, at titanium plate surface melting depending on the accumulated laser radiation energy, the surface color might be changed from bright yellow to red and deep-blue colors. In the paper<sup>2</sup>, the data on titanium surface oxidation in atmospheric pressure air at pulsed Nd:YAG lasing are presented. The laser operated at the wavelength of 1,064 nm, average radiation output of 60 W at 30 kHz. Several samples were treated by accumulation of different laser pulses per unit of square. The experiments were carried out at accumulated laser energy from 54 up to 294 J/cm<sup>2</sup>. The characteristics of the treated samples and different colors appeared were studied using various measurement techniques. Morphology analysis by scanning electron microscopy has revealed that melting and second solidification occurs during laser beam action in the whole range of exposure values. Moreover, at more high values of the accumulated fluxes the craters are forming. Measurements of spectral reflection allowed to determine chromatic coordinates corresponding to different

---

\* VFT@loi.hcei.tsc.ru; phone: (+7 382-2) 258685; fax: (+7 382-2) 259410; http:// [www.hcei.tsc.ru](http://www.hcei.tsc.ru); High Current Electronics Institute, 4, Akademicheskoy Ave., Tomsk 634055, Russia

colors observed on the samples. X-ray diffractometry has shown that at low exposure values no oxidation occurs but crystallites orientation change to the characteristic of powders distribution takes place. Diffractograms at higher accumulated fluences reveal the formation of basically  $\text{Ti}_2\text{O}$  and  $\text{TiO}$  crystalline phases among the oxides, which show a monotonic increase in their content with increase of irradiation rate. Other phases such as  $\text{TiO}_2$  either in rutile or anatase crystalline structures, or  $\text{Ti}_2\text{O}_3$  were identified through Raman spectroscopy. The low Raman signal levels and absence of those phases in most of the diffractograms points to that their contents is essentially smaller than that of  $\text{Ti}_2\text{O}$  and  $\text{TiO}$ . Besides that, the change of signal levels as a function of the accumulated laser fluence is non-monotone. The comparison of the compositional analyses with color distribution observed shows that there is some correlation between the onset of the different colors and changes in the composition of samples<sup>2</sup>.

The above presented results testify to the possibility to use the change of titanium surface color at heating by laser irradiation in the open air to obtain dot raster images (even colored ones). For this, as an image carrier either a thin titanium layer (silver color) or titanium dioxide (white) at the paper surface can be used. From this reasoning, we have carried out experiments on determination of color change conditions for thin titanium foils irradiated by pulsed IR laser.

Presently, from the world data available on interaction of laser radiation with metal and dielectric surfaces and development of experimental diagnostics techniques by itself it is allowed to raise a reverse question, i.e., restoration of laser radiation energy spatial distribution through surface imprint. Using imprints, it is also possible to make an express diagnostics of multi-layer surface coatings. With this in mind, we have made the detailed morphology of imprint of the pulsed HF-laser interaction with carbon steel surface through atomic force microscope.

## 2. EXPERIMENTAL EQUIPMENT AND TECHNIQUES

Based on the developed at the HCEI e-beam accelerators and powerful electrical schemes, a succession of lasers based on high pressure gases was created<sup>3-8</sup>. For the experiments on laser radiation interaction with matter from the point of view of high power, high energy and high efficiency, the  $\text{XeCl}^*$ ,  $\text{CO}_2$  and HF molecules based lasers and lasers on atomic transitions of Xe were chosen. Radially convergent and planar e-beam based accelerators and set-ups with self-sustained discharge and e-beam-initiated discharge were used as excitation sources. Maximal radiation output energy in UV spectral range of up to 2 kJ has been obtained at  $\lambda=308$  nm for 600-l e-beam pumped  $\text{XeCl}$ -laser<sup>6,7</sup>. Using the same experimental set-up but with Ar-Xe ( $\lambda=1.73$   $\mu\text{m}$ ) and He-Ar-Xe ( $\lambda=2.03$   $\mu\text{m}$ ) mixtures, the output lasing as 100 and 50 J, correspondingly, has been achieved. Laser radiation output energy of 110 J at  $\lambda=308$  nm and of 90 J at  $\lambda=249$  nm were demonstrated using the set-up with a radially convergent e-beam and active volume of 30 liters and laser radiation aperture of 20  $\text{cm}^3$ . Choice of radially convergent e-beam pumping appeared to be successful for excitation of non-chain HF laser. The output energy of generation up to 200 J with efficiency up to 10 % in reference to the loaded into the gas e-beam energy has been obtained at the HF molecule transition at  $\lambda \sim 2.8$   $\mu\text{m}$ <sup>3,4</sup>. The average output laser radiation up to 1 kW was realized using  $\text{CO}_2$  – laser pumped by e-beam preionized discharge at pulsed repetition rate (p.r.r.) of 50 Hz<sup>7</sup>. The use of inductive energy storage for pumping of non-chain discharge HF laser allowed to obtain lasing with the efficiency up to 5.5 % in reference to the input energy in gas, and use of zeolite absorber allowed to increase the gas mixture lifetime up to 1000 pulses<sup>7,8</sup>. Use of the generator based on inductive energy storage in order to form a prepulse in the gas discharge  $\text{XeCl}$  laser allowed to form a high homogeneity discharge and to increase duration of oscillation up to 450 ns at output energy up to 1.1 J and total efficiency of 2.2 %. The main parameters of the experimental laser set-ups are presented in the Table 1.

In our experiments we used two laser set-ups. The set-up № 1 was based on the e-beam preionized discharge laser<sup>7</sup>. Active gas volume of 72.3-2.4  $\text{cm}^3$  was bounded by a copper electrode and a steel mesh protecting the electron accelerator exit foil window. The e-beam parameters were as follows: duration of 4 ns, total current behind the foil of 6 kA, and average energy of electrons behind the foil was of  $\sim 150$  keV. The bank of capacitors with total capacitance of 0.2  $\mu\text{F}$  was situated directly in the gas chamber being charged up to 10-12 kV. The resonator consisted of a flat mirror with aluminum coating and a parallel-plane plate KRS-5 as output window. The parallel-plane resonator provided laser radiation divergence of about 1,6 mrad. Water cooling systems of the output foil window and operating mixture circulation at flow velocity of about 10 m/s allowed operation at p.r.r. of up to 50 Hz. The mixture Ar:Xe=100:1 at pressure of 1 atm was used. The main part of laser energy was radiated at  $\lambda = 1.73$   $\mu\text{m}$ .

The laser provided an impulse energy as 10-15 mJ at duration  $\sim 320$  ns and average power of 70 and 300 mW at p.r.r. of 10 and 25 Hz, correspondingly.

As the second set-up we used HF discharge non-chain chemical laser<sup>5,8</sup>. The active volume was  $60 \cdot 2.3 \cdot 1$  cm<sup>3</sup> pumped through the two-circuit scheme preionized by the surface discharge from under the mesh which is one of the electrodes. The bank of capacitors with total capacitance of 64 nF charged up to 40 kV was the main storage, with this the peaking capacitor was 23 nF. The laser resonator consisted of a flat steel mirror and a parallel-plane plate either KRS-5 or CaF<sub>2</sub> as an output window. Laser pulse energy was of 1.5 – 2.0 J at pulse duration of  $\sim 350$  ns. HF-laser could also be operated in a pulsed repetition mode with frequency of up to 5 Hz. Zeolite used as an absorbent for HF molecules produced in discharge allowed to achieve stable energy parameters of laser pulses with decrease for 10-15% at  $10^3$  turns on at 1-2 Hz.

Laser radiation energy and average power were measured by a calorimeter IMO-2N and pyroelectric sensor PE-25 (OPHIR Opt.) calibrated in the measured optical range with an accuracy of 5%.

In order to investigate the irradiated surface we used optical microscopes of MBS-10 type (maximal magnification is 100x) and MMR-4 type (maximal magnification is 1300x). For morphology analysis of the samples a scanning probe microscope "Solver P47" (produced by NT-MDT, Russia) was used. Relief imaging of the surface was obtained in the mode of contacting atomic-force microscopy. The probe force affected the sample was equal to  $1.7 \cdot 10^{-7}$  N, and the curvature radius of the probe was about 10 nm. The sample was continuously scanned along X-axis with a velocity of  $4.77 \cdot 10^{-4}$  m/s and moved discretely along the Y-axis with frequency of 2 Hz and lead of  $4.751 \cdot 10^{-8}$  m.

### 3. INTERACTION OF IR RADIATION WITH TITANIUM FOIL SURFACE

In the experiments the titanium foils of 8, 13 and 50  $\mu$ m in thickness were used. Focusing was realized using the lens made of BaF (F=123 mm), the diameter of the focal spot made about 300  $\mu$ m. In the pulsed repetition mode (pulse frequency was 25 Hz, average laser power was 250 mW) the thin foils of 8 and 13 mm in width had been destroyed in about 5 s (accumulated energy density was  $q = 1,063 \cdot 10^3$  J/cm<sup>2</sup>) or 300 pulses in a single mode ( $q = 1,786 \cdot 10^3$  J/cm<sup>2</sup>) and 4 min ( $q = 51.02 \cdot 10^3$  J/cm<sup>2</sup>), correspondingly. The rupture occurred in the area of the maximal energy of the focal spot due to titanium foil heating up to temperatures enough for plastic deformation and foil break-through, obviously, due to laser plasma pressure in the pulse-repetition mode. With this, the foil broken edges turned around away from the laser radiation. The more thick foil of 50  $\mu$ m had not been heating up downward totally and it was destroyed. Such a mechanism of the foil break-through can explain reasons for absence of effect at low-frequency operation in the case of using the foil of 13  $\mu$ m in thickness and in the case of 50  $\mu$ m-foil. At low-frequency operation (p.r.r. was  $\leq 1$  Hz) the impulse energy within the time between pulses had been dissipated (re-emission, heat conduction) and the foil was not heated up to the temperature needed.

The surfaces of all the samples at change of accumulated laser energy due to exposure time and p.r.r. variation were observed to change color. Figure 1 presents photos of the titanium foil surface at different irradiation regimes. With not high energies accumulated by titanium foil surfaces (both in single mode and at not high p.r.r.) the foil surface remelting occurs. In certain conditions (50 mW output power, 25 Hz, 4 min, 50  $\mu$ m-foil), after cooling the remelt surface was observed as cracked areas that points to the fact that internal stress forces occurred in the foil. With increasing of accumulated energy ( $q = 2,125 \cdot 10^3$  J/cm<sup>2</sup> at 25 Hz, or  $q = 1,45 \cdot 10^3$  J/cm<sup>2</sup> at 10 Hz), Fig. 1(a,d), the surface of the titanium 13  $\mu$ m-foil becomes yellow. Further increase of energy value ( $q = 4,25 \cdot 10^3$  J/cm<sup>2</sup> at 25 Hz and  $q = 1,78 \cdot 10^3$  J/cm<sup>2</sup> at 10 Hz) brought to color change from yellow to dark-blue in the imprint center, Fig. 1(b,e). And lastly, at accumulated energy of  $q = 6,38 \cdot 10^3$  J/cm<sup>2</sup> the whole imprint surface gains dark-blue color, Fig. 1(c,f). The basic data are presented in the Tab.2. Here the data on oxide film composition obtained by A. Perez del Pino, et al.<sup>2</sup> are also shown.

For comparison purposes, an experiment on UV laser radiation effect on titanium foil of 50  $\mu$ m in thickness was made. A discharge exciplex laser "Foton"<sup>7</sup> with the wavelength of 222 nm (KrCl), pulse duration of 20 ns and pulse energy of 35 mJ was taken. In some experiments the energy of lasing decreases up to 3 mJ due to using a

diaphragm. The laser could operate in a single pulse regime or at p.r.r. of 1 Hz. The radiation focusing was realized using quartz lens with focal distance of 10 cm. In those regimes tried (single pulse regime, pulsed repetition regime with frequency of 1 Hz) there was a crater followed after on the titanium foil surface with melt bottom of the silver color. At multiple irradiation (over 5 pulses) there the bands of yellow-orange and blue colors appeared around the crater. The melt surface of the crater represented by itself a wavy structure, most clearly expressed at multiple laser action (10-15 pulses). The colored bands around the crater are probably determined by deposition of titanium oxides, having been evaporated by laser radiation from the crater and reacted with oxygen from air. It must be noted that those colored bands repeated in shape the areas radiated by the part of UV radiation with greater divergence.

#### 4. TOPOLOGY OF STEEL SURFACE AFTER INTERACTION WITH POWERFUL IR LASER RADIATION

The carbon steel sample 4140 was placed in the focal plane of lens ( $F = 123$  mm). After irradiation by 10 pulses from HF-laser (p.r.r. is 0.5 Hz) a crater with the area of  $1 \times 0.5$  mm<sup>2</sup> formed on the steel surface (see Fig. 2). Figure 2 also presents the photos made using optical microscope of the 5 separate crater zones differed in surface topology. Surfaces of the far zones № 4 and 5 represent by itself solidified metal splashes carried away from the central zones melt by laser irradiation. The splashes are directed outward the center of crater, their sizes being decreased as moving away from the center. Measurements were carried out by reweighing of the sample, which had many not overlapping single pulse imprints. It was shown that within a single laser impulse about  $4 \cdot 10^{-4}$  g/cm<sup>2</sup> of metal was removed from the sample surface. Zones №2 and 3 are situated closer to the crater center and present by itself the areas of solidified metal with wavy surface. Figure 3(a,b) shows the scanning results obtained in those areas using atomic force microscope. Heights of irregularities (waves and drops of solidified metal) in zone №3 made up to 650 nm that is the most high value for all the crater areas. There are separate drops seen which have transversal sizes of 2–3 µm. In zone №2, irregularities height does not exceed 250–300 nm and separate drops are practically absent. Besides, on the image obtained by scanning the surface in zone №2 using atomic force microscope there is a fine grain structure, see Fig. 3(b). Transversal sizes of grains are 400–800 nm, they vary above the metal surface by 15–30 nm. In the central crater zone, i.e. zone №1, irregularities also do not exceed the height of 300 nm and the grain structure is observed. Differed from zone №2, these grains are somewhat smaller in size (transversal size is 200–500 nm, the height above the surface is 10–15 nm). Big grains are also observed, see Fig. 3(c). Figure 4 presents a surface profilogramme of zone №1 showing a part of coarse grains. Height of the coarse grain decreases from the center to edges for about 40 nm overlaying metal surface totally for 100–120 nm. Cross-section size of such a coarse grain is well seen in Fig. 4 (zone №1) and makes 50 – 60 µm.

#### 5. DISCUSSION AND CONCLUSION

While comparing our results obtained for thin foils with experimental results obtained for 1-mm width plates<sup>2</sup>, the following conclusions may be done. Effect of titanium surface modification is determined by temperature and is dependent on supply heating rate and the heat dissipation rate of the sample. The values of the specific laser energy accumulated by surface at which modification occurs in our experiments exceed by several orders the values reported by A. Perez del Pino, et al.<sup>2</sup>. It may be explained that in the experiments<sup>2</sup>, at high p.r.r. (30 kHz) the surface temperature becomes increased with each following impulse, and though the major thickness of the sample as compared with foil provides a high heat removal rate, the heating up occurs more efficiently. Other fact was that the reflection factor of laser radiation by the metal surface becomes lower with increase of temperature of the sample. Moreover, in our experiments, the laser radiation pulse energy exceeded the value taken by A. Perez del Pino, et al. by 3–5 factors that led to much higher absorption of laser radiation in the plume of laser plasma and evaporated target matter.

In order to produce colored oxide film on a thin titanium foil through one laser radiation impulse we need to have longer pulse duration, such as, to have (at energy enough) the surface heating up to necessary temperatures and keeping such temperature within a certain time needed for chemical reactions to take place. For determination optimal parameters of laser impulse it is necessary to carry out additional experiments and calculations.

Surface structure formation in zone №2 occurs following two mechanisms: 1) melting and solidification of the metal resided in the given zone directly; 2) cooling and solidification of the metal removed under influence of hydrodynamic forces from zone №1 due to intensive boiling. In distinction to zones №3 and №4, where the melt metal removed out the crater center is being cooled down at a comparatively cold surface, in zone №2 the initial surface temperature and evaporated metal correlate, owing to which much slower metal cooling down occurs resulting in fine grained structure formation. The similar fine-grained structures identified as grains of  $\gamma$ -iron were obtained at carbon steel surface melting by pulsed high-energy electron beam<sup>9</sup>. In zone №1, the surface temperature during a laser radiation pulse is the highest one and the main processes occurred are intensive boiling and metal evaporation. In this case an initial ferropearlite structure develops with a characteristic morphology of solidification for each phase. It is supposed that the large smooth grain in the Fig. 2(a) is a ferrite one. There are other pearlite grains possessing typical fine-grained structure resided around it.

A more accurate identification of the structures formed on the carbon steel surface affected by laser radiation pulse demand further additional experiments.

### ACKNOWLEDGEMENTS

The work has been fulfilled being supported by ISTC, the Project No 1206.

### REFERENCES

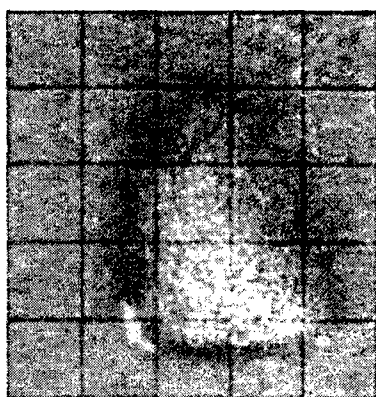
1. V.S. Kovalenko, *Lazernaja tekhnika i tekhnologija*. – K.: Vishcha shkola. Golovnoje izdatel'stvo, 280 p., 1989 (in Russian).
2. A. Perez del Pino, P. Serra, J.L. Morenza, "Oxidation of titanium through Nd:YAG laser irradiation", *Abstracts of the 6-th Intern. Conf. on Laser Ablation COLA'01*, October 1-5, 2001, Tsukuba, Japan, p. 228.
3. E.N. Abdullin, A.M. Efremov, B.M. Koval'chuk, V.M. Orlovskii, A.N. Panchenko, V.V. Ryzhov, E.A. Sosnin, V.F. Tarasenko, I.Yu. Turchanovskii, "Laser based on an SF<sub>6</sub>-H<sub>2</sub> mixture pumped by a radially converging electron beam", *Quantum Electronics*, **24**, №9, pp. 761-765, 1997.
4. E.N. Abdullin, A.M. Efremov, B.M. Koval'chuk, V.M. Orlovskii, A.N. Panchenko, E.A. Sosnin, V.F. Tarasenko, A.V. Fedenev, "Powerful HF laser pumped by e-beam initiated non-chain chemical reaction", *Pis'ma v JTF*, **23**, № 5, pp.58-64, 1997 (in Russian).
5. V.F. Tarasenko, S.B. Alekseev, M.V. Erofeev, V.M. Orlovskii, *Proc. of the Int. Conf. LASERS 2000*, Ed. By V.J. Corcoran and T.A. Corcoran, STS Press, McLean, VA, pp.317-322, 2001.
6. E.N. Abdullin, S.P. Bugaev, A.M. Efremov, V.B. Zorin, B.M. Koval'chuk, V.V. Kremnev, S.V. Loginov, G.A. Mesyats, V.S. Tolkachev, P.M. Shanin, "Electron accelerators based on Marx generator with vacuum insulation", *Pribori i Tekhnika Eksperimenta*, № 5, pp.138-141, 1993 (in Russian).
7. V.F. Tarasenko, E.H. Baksht, A.V. Fedenev, V.M. Orlovskii, A.N. Panchenko, V.S. Skakun, E.A. Sosnin, "Ultraviolet and infrared lasers with high efficiency", *Proc. of the Int. Conf. High Power Laser Ablation, SPIE Vol. 3343*, pp.715-724, 1998.
8. V.F. Tarasenko, S.B. Alekseev, M.V. Erofeev, V.M. Orlovskii, "Electrodischarge HF-lasers on H<sub>2</sub>-SF<sub>6</sub> mixture", *Proc. of the Intern. Conf. LASERS-2000*, Albuquerque, New Mexico, Dec. 4-8, 2000, STS Press, McLEAN, VA, pp. 317-323, 2001.
9. V.B. Markov, V.P. Rotshtein, "Thermal and strain-wave mechanism of hardening of carbon steel at effect of high-energy high-current e-beam", *Fizika i Khimija Obrabotki Materialov*, **6**, pp. 37-41, 1997 (in Russian).

Table 1. Characteristics of laser set-ups.

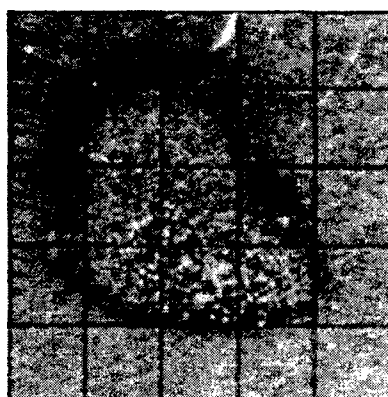
Set-ups	Pumping technique, Active medium, P.r.r.	Transitions, Wavelengths, Gas mixture, pressure	Pulse duration, Energy, Efficiency	Notes
"DM"	Electron beam, $j = 40 \text{ A/cm}^2$ , 600 l, aperture $D = 60 \text{ cm}$ single pulse regime	XeCl, 308 nm, Ar-Xe-HCl, $p=2.5 \text{ atm}$	300 ns, 2000 J,	[6], [7]
		Xe, 1.73 $\mu\text{m}$ , 2.03 $\mu\text{m}$ , Ar-Xe, He-Ar-Xe	300 ns, 100 J, 50 J, 1-2 %	[7]
"Coaxial"	Electron beam, $I = 5 - 500 \text{ A}$ , 200 kV 20 l, aperture $D = 20 \text{ cm}$ 0.1 – 50 Hz	Xe, 1.73 $\mu\text{m}$ , 2.03 $\mu\text{m}$ , Ar-Xe, He-Ar-Xe $p = 1.0 - 1.5 \text{ atm}$	10 – 1000 $\mu\text{s}$ 6 J, 2 %	Water cooling of the foil [7]
"ELON - 1M"	Electron beam, $j = 40 \text{ A/cm}^2$ , 30 liters, aperture $D = 20 \text{ cm}$ single pulse regime	XeCl, 308 nm, Ar-Xe-HCl, $p=2.5 \text{ atm}$	300 ns, 110 J, 5.5 %	[7]
		Xe, 1.73 $\mu\text{m}$ , 2.03 $\mu\text{m}$ , Ar-Xe, He-Ar-Xe	700 ns, 16 J, ~ 2 %	
		HF, (non-chain) ~ 2.8-3 $\mu\text{m}$ , SF <sub>6</sub> -H <sub>2</sub>	700 ns, 200 J, 11 %	[3,4]
"Cascade"	E-beam initiated discharge, 72x3x2.4 cm <sup>3</sup> , 0.1 – 50 Hz	CO <sub>2</sub> , 10.6 $\mu\text{m}$ , N <sub>2</sub> -CO <sub>2</sub> -H <sub>2</sub>	50 ns – 8 $\mu\text{s}$ , 30 J, 1 kW	Gas cooling and circulation system [7]
"LIDA-T"	Discharge, 3.5x1.5x60 cm <sup>3</sup> , 5 Hz	XeCl, 308 nm, Ar-Xe-HCl, $p=2.0 \text{ atm}$	100-450 ns, 0.2 – 1.0 J,	Inductive energy storage generator [7]
		HF, (non-chain) ~ 2.8-3 $\mu\text{m}$ , SF <sub>6</sub> -H <sub>2</sub>	350 ns, 2 J, 2.9 %	[5,8]

Table 2. Characteristics of titanium foil surface modification (foil thickness is 13  $\mu\text{m}$ ) with dependence on the laser radiation energy accumulated at different regimes. Composition of oxide coatings was taken from [2] for similar experimental conditions.

Surface modification	P.r.r.	Time of treatment	Laser radiation energy accumulated, J/cm <sup>2</sup>	Composition of the surface coating [2]	Notes
Remelting	10 Hz	10 s	~ 0,6·10 <sup>3</sup>	Crystallites orientation similar to that of powders	On treatment at low average power the surface is being cracked
Remelting	1 Hz	10 pulses	~ 0,059·10 <sup>3</sup>	The same	
Yellow color	10 Hz	20 s	1,45·10 <sup>3</sup>		Probably due to titanium nitride
Reddish-yellow color	25 Hz	10 s	2,13·10 <sup>3</sup>	a-Ti <sub>2</sub> O <sub>3</sub> + TiO <sub>2</sub> (rutile)	
Appearance of dark blue color traces	10 Hz	30 s	1,78·10 <sup>3</sup>	a-Ti <sub>2</sub> O <sub>3</sub> + TiO <sub>2</sub> (rutile)	In the spot center against a background of yellow
Appearance of dark blue color	25 Hz	20 s	4,25·10 <sup>3</sup>	a-Ti <sub>2</sub> O <sub>3</sub> + TiO <sub>2</sub> (rutile)	In the spot center against a background of yellow
Dark blue color	25 Hz	30 s	6,38·10 <sup>3</sup>	c-Ti <sub>2</sub> O <sub>3</sub> + TiO <sub>2</sub> (rutile)	The spot is uniform in color
Hole break- through	25 Hz	4 min	51.02·10 <sup>3</sup>		Edges of hole are melt and forced apart



a



b



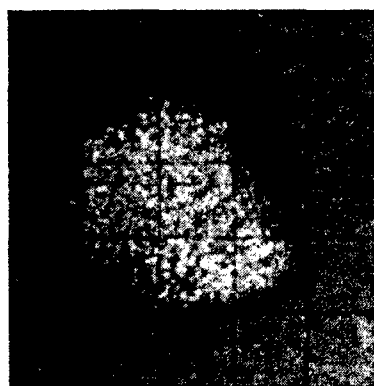
c



d



e



f

Fig.1. Photo of the titanium foil surface (thickness of foil is  $13\text{ }\mu\text{m}$ ) after irradiation by Ar-Xe laser. (a,b,c) – an average power of 250 mW at p.r.r. of 25 Hz, (d,e,f) – an average power of 70 mW at p.r.r. of 10 Hz. Time of treatment is 10 s (a,d), 20 s (b,e), 30 s (c,f). The side of the grid square is equal to  $140\text{ }\mu\text{m}$ .



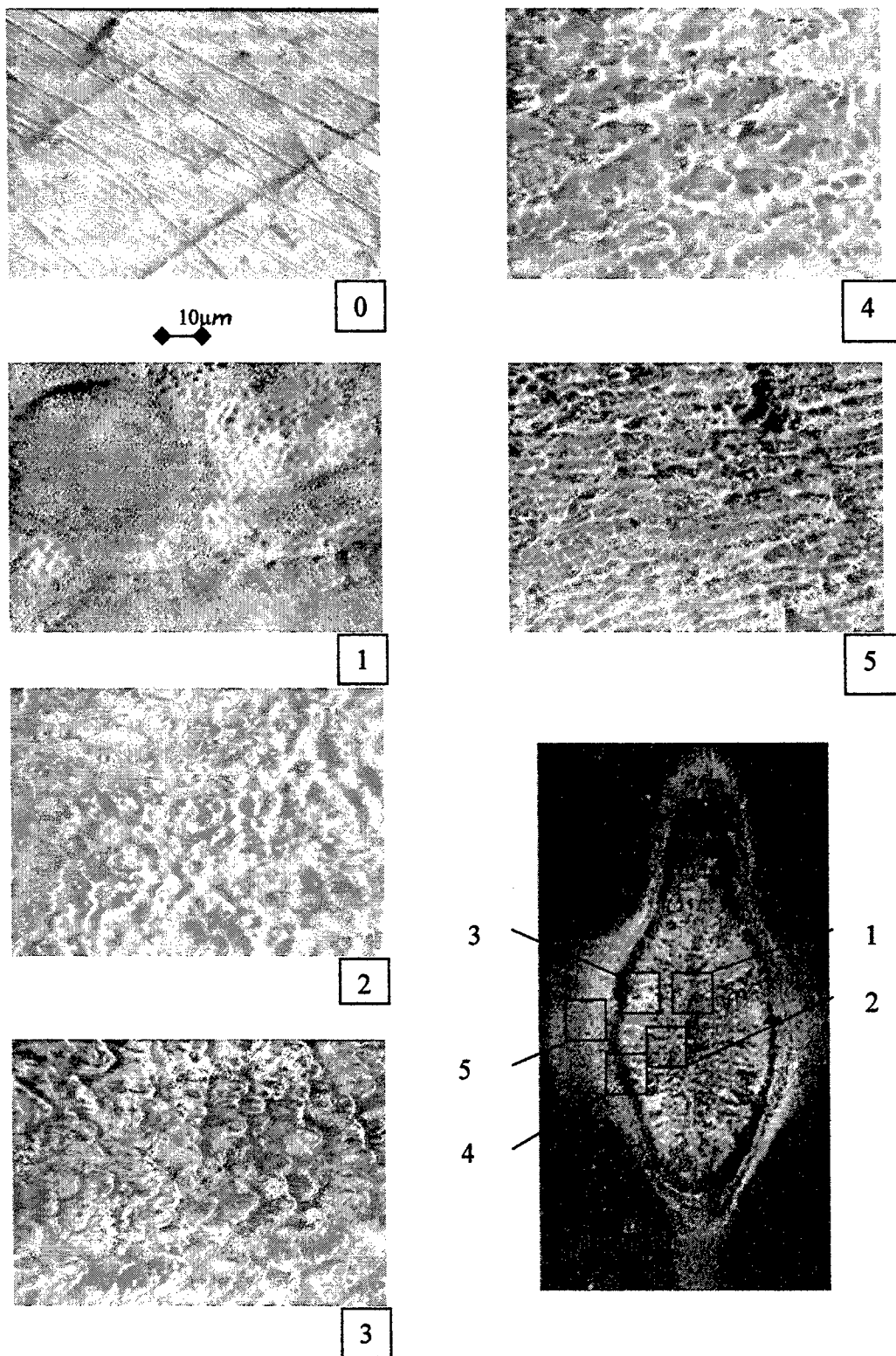


Fig.2. HF-laser print on the 4140-steel surface (10 pulses) and magnified images of distinguished zones.

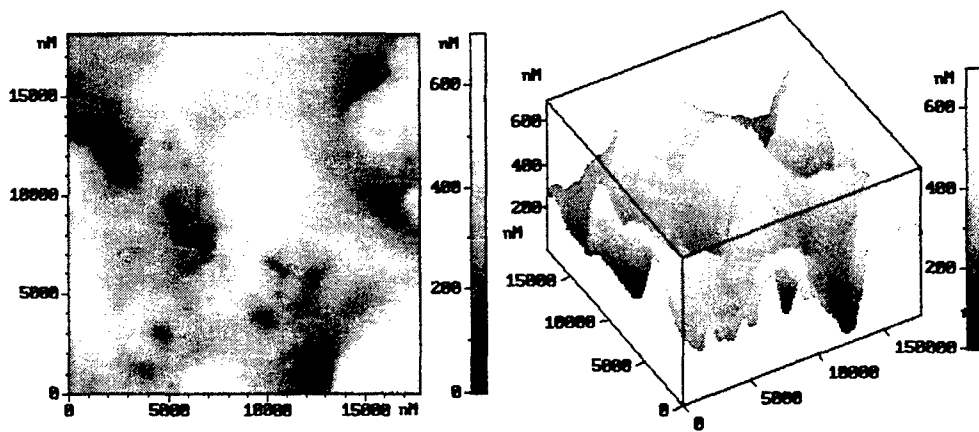


Fig. 3(a). The metal surface observed after laser action (zone №3).

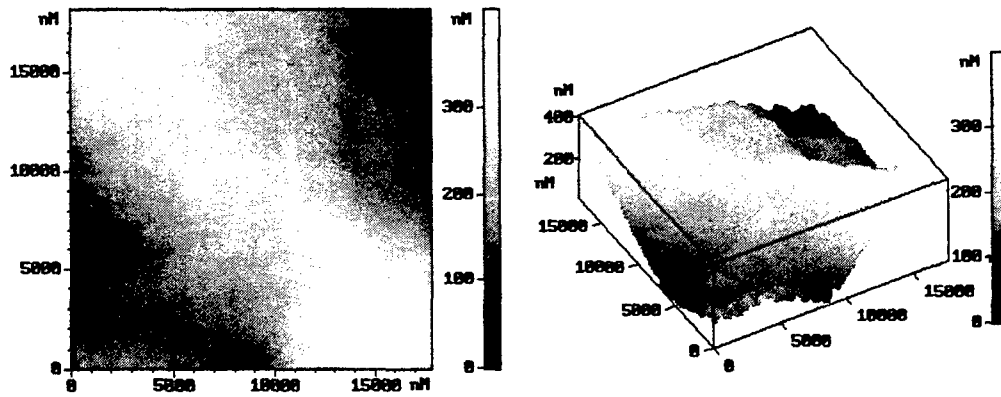


Fig. 3(b). The metal surface observed after laser action (zone №2).

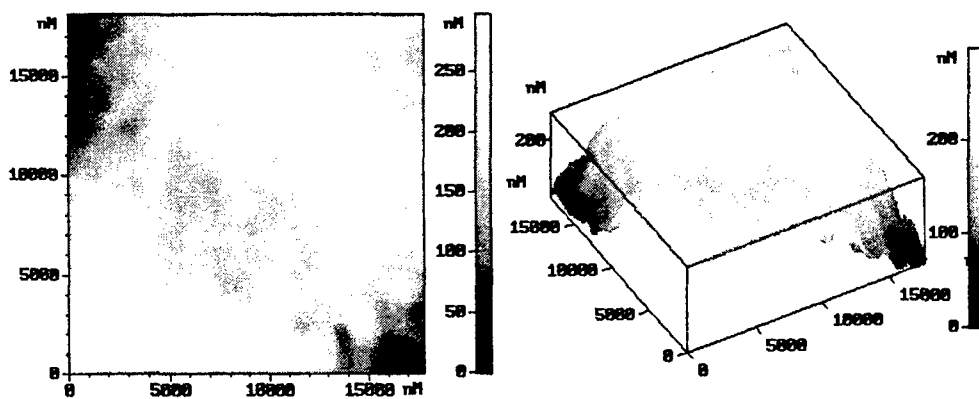


Fig. 3(c). The metal surface observed after laser action (zone №1).

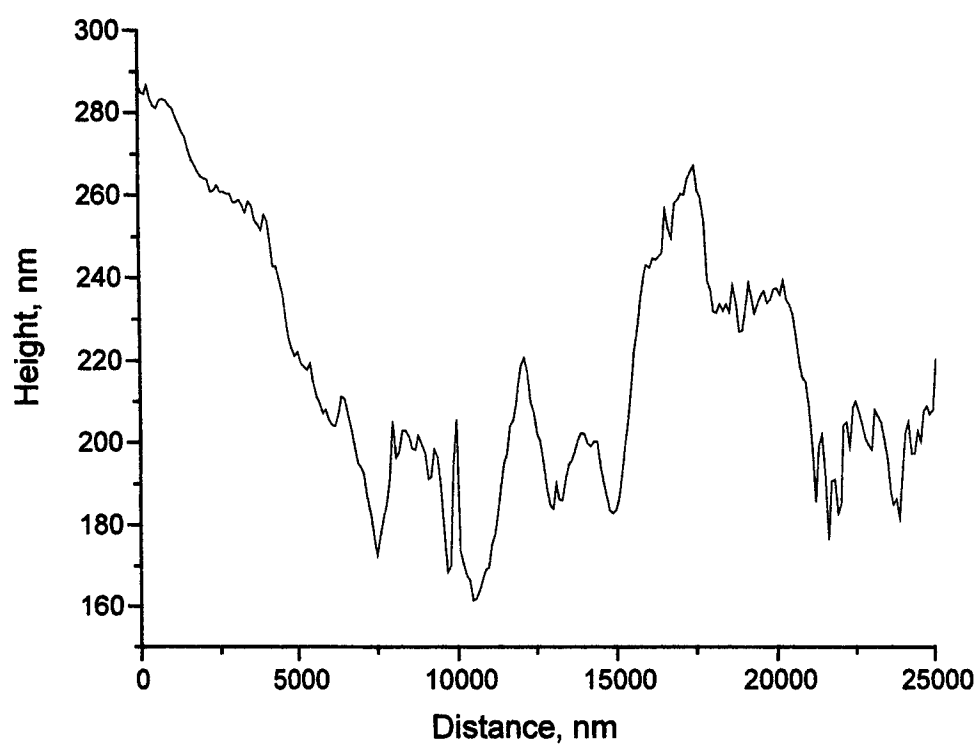


Fig. 4. Profilogramme of the crater surface in zone № 1 (along the diagonal line of Fig. 3(c) from the left to right, from the down to top) obtained using the software of the atomic force microscope.